Experimental Protocol for High-Pressure Gasoline-Spray Drop-Size Distribution Measurements by Using Laser-Diffraction Technique

Christophe Dumouchel, P. Yongyingsakthavorn, J. Cousin

Experimental Protocol for High-Pressure Gasoline-Spray Drop-Size Distribution Measurements by Using Laser-Diffraction Technique

C. Dumouchel[1], P. Yongyingsakthavorn[2,*], J. Cousin[1]

[1] CNRS UMR 6614 – CORIA, Université et INSA de Rouen, Avenue de l'Université, B.P. 12
76801 Saint Etienne du Rouvray, France
[2] Department of Mechanical Engineering, King Mongkut's University of Technology North Bangkok, Bangkok, Thailand
[*] Corresponding author: pisit_y@hotmail.com

Abstract: *This paper reports an experimental investigation on the practical use of a laser-diffraction instrument, the Malvern Spraytec 2007, to characterize highly transient sprays produced by a high-pressure GDI injector. The sprays are large, composed of very small drops, dense and heterogeneously distributed in space. These characteristics may be at the origin of undesirable effects (beam steering, vignetting and multiple light scattering) that bias the measurements. The manifestation of these effects is experimentally identified and solutions to erase their influence are provided. A particular attention is paid on the multiple light scattering effects. A correction procedure is developed. It consists in determining a correction factor series to be applied on the normalized light intensity distribution. The corrected drop-size distributions are calculated from the new light intensity distribution. Furthermore, this procedure succeeds in correcting vignetting effects. Despite the correction procedure is applicable for the present operating conditions only, this work defines a clear protocol to apprehend laser-diffraction spray characterization in severe operating conditions and to establish a correction procedure if required. Among other results, it is emphasized that the combination of the Spraytec and the correction procedure performances allows the temporal evolution of the drop-size distribution during an injection and cycle-to-cycle spray drop-size distribution variations to be determined. Such information is of paramount importance and the Spraytec is probably the sole instrument able to provide it.*

Keywords: Spray, Drop size distribution, Laser diffraction, Light multiple scattering, GDI injector

1. INTRODUCTION

The laser diffraction technique provides a line of sight average measurement of the drop-size distribution. A part of the laser beam that passes through the spray is diffracted. In the forward direction, the light falls on a Fourier transform lens: the undiffracted light is focused onto a point on the axis in the focal plane and the diffracted light forms a far-field Fraunhofer pattern around this central spot. The ratio of the undiffracted light intensity I to the incident light intensity I_0 provides the transmission T of the measurement, i.e.,: $T = I/I_0$. A mathematical inversion procedure based on the Fraunhofer diffraction theory calculated the volume-based drop-size distribution that had the same diffraction pattern as the one recorded on a detector. Over the past years laser-diffraction instruments have been modified and improved. For the Malvern Spraytec series, it is now based on the Lorenz–Mie theory accounting for the contribution to the angular light energy distribution of refraction, which improves the instrument performances when measuring very fine sprays [1]. Furthermore, the mathematical inversion also includes a patented multiple scattering algorithm.

This work aims to present an experimental protocol when laser light diffraction measurements are performed in severe operating conditions, i.e., large, dense, highly transient and inhomogeneous sprays. The sprays investigated are those produced by a gasoline direct-injection (GDI) device. First, the undesirable effects of light multiple scattering, vignetting and beam steering are identified. Second, an empirical correction model is developed to correct the measurements from vignetting and light multiple scattering effects. The application of this model allows the Malvern correction algorithm to be tested and the performances of the GDI injector to be determined.

2. EXPERIMENTAL SETUP AND DIAGNOSTICS

The liquid used is Exxsol D40 (density ρ = 776 kg/m^3, surface tension σ = 24.7 mN/m, kinematic viscosity μ = 1.3 mm^2/s). Its temperature is maintained at 18 ± 2 ºC. An injection pressure ΔP_i can be regulated from 0.5 to 20 MPa by a high-pressure sensor. The injector investigated is a non-swirl outward opening GDI injector that produces a hollow conical issuing flow without imposing any internal swirling motion. The Engine Control Unit (ECU) controls the injection time and frequency as well as the actuation energy that imposes the needle stroke. Throughout the study this time is equal to 2 ms. The injection frequency is maintained at 0.2 Hz and the needle stroke energy at 63% of the full scale corresponding to a needle stroke of the order of 35 μm.

The Malvern Spraytec 2007 is used (wavelength = 632.8 nm, laser baem diameter = 10 mm). A series of 36 diodes equips the receiver. The collecting lens has a focal length equal to 300 mm (diameter range is 0.5–600 μm). The spatial arrangement of the Spraytec is schematized in Fig. 1. The distances d_I, d_D and L_s indicated are equal to 50, 180 and 84 mm, respectively. These distances are kept constant except otherwise mentioned. The measurements are performed at the highest acquisition rate of 10 kHz.

Fig. 2 shows the temporal evolution of transmission for several injections for ΔP_i = 10 MPa. It is seen that the evolution slightly differs from one injection to another. To avoid this problem, we decided to average the measurement on 25

injections in analysis. The evolution of the average transmission is also shown in Fig. 2. Minimum transmissions T_{min}, light intensity distributions and drop-size distributions presented and analyzed in this paper all result from this averaging process.

Vignetting and laser beam steering are two undesirable phenomena that affect laser-diffraction measurements. To quantify vignetting effects, measurements of the left portion of the spray only at different working distance of 88, 138 and 218 mm are performed (d_D = 130, 180 and 260 mm, see Fig. 1). We found that vignetting affects on diode 36 for d_D = 180 mm and on diodes 34–36 for d_D = 260 mm. The distance d_D was kept at 180 mm throughout the experimental work, since a shorter distance was inappropriate because of drop impaction on the lens at high ΔP_i. Thus, diode 36 always affected is ignored in analysis whereas diodes 34 and 35 are going to be used to correct the right-spray portion. Beam steering effect is the manifestation of light scattered because of a refractive index gradient in the gas phase, which deviates light at small angles leading to overestimating the big drop population. To avoid the bias caused by beam steering, Malvern recommends ignoring the first diodes. The number of diodes to be ignored is a function of the operating conditions. In the present work, we found that ignoring the nine first diodes was required to ensure the disappearance of the big drop supplementary peak for all operating conditions. In conclusion, spray drop-size characteristics are calculated on the basis of the intensity distribution collected from diode 10 to 35.

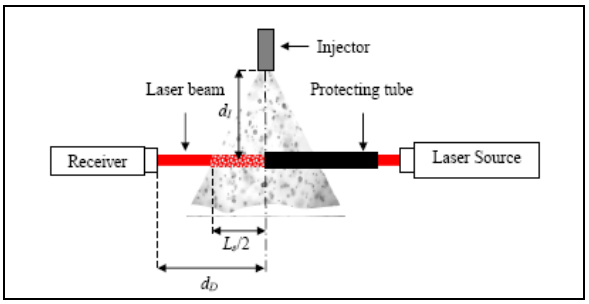

Fig. 1 Malvern Spraytec arrangement

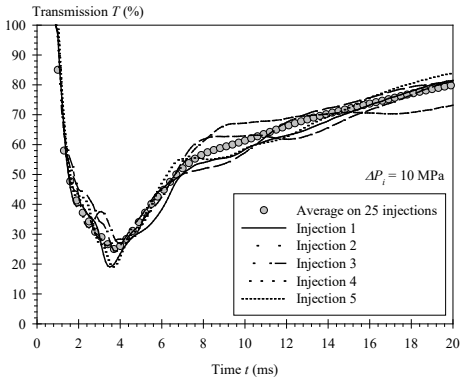

Fig. 2 Temporal evolution of the transmission during the injection. Influence of the injection event (ΔP_i = 10 MPa).

3. RESULTS

3.1 Influence of light multiple scattering and vignetting effects

As several investigations [2-9], an influence of multiple light scattering cannot be negligible when transmission is less then 40%. When both spray portions are measured (full spray measurement) this limit is reached for an injection pressure equal to 6 MPa. This pressure becomes 11 MPa when one portion of the spray is measured (half-spray measurement). Therefore, in the range of pressure of interest [15 MPa; 20 MPa] light multiple scattering effects are expected. To identify these effects, comparing full and half-spray measurements provided that the half-spray measurement transmission is equal to or greater than 40% is performed. This protocol makes sense if the protecting tube does not affect the spray characteristics and if these characteristics are axisymmetric. Therefore, two preliminary tests are performed.

The first test consists in comparing the transmissions of full and half-spray measurements. For spray axisymmetry, the transmission T' of the half-spray measurement is related to the full spray measurement transmission T by: $T' = \sqrt{T}$ (see [2]). We found that the agreement between the calculation and the measurements is acceptable. The second test consists in comparing the full and half-spray drop-size distributions for an injection pressure that guarantees no light multiple scattering effects for both measurements. Such comparisons are presented in Fig. 3 for ΔP_i = 1 MPa and 5.47 MPa. The results show that half and full-spray drop-size distributions agree very well. The measurements were conducted along several diameters of the spray by rotating the injector and the same results are obtained. Note that the impact of vignetting effect identified above on full-spray measurement is undetectable at these low ΔP_i. These preliminary tests demonstrate that the protecting tube introduces a negligible perturbation and that the spray drop-size distribution is axisymmetric enough to consider the half-spray distribution representative of the whole spray distribution. The presence of light multiple scattering are observed by considering the evolution of characteristic drop diameters and of the light intensity distribution with the transmission. Fig. 4 shows the full-spray diameter/half-spray diameter ratios as a function of the full-spray transmission T. For T > 40%, the diameter ratios are of the order of 1 as expected. Then, when T is between 40% and 14%, the ratios increase a bit. When the transmission further decreases, the $D_{v0.5}$, $D_{v0.9}$ and D_{43} ratios mainly decrease whereas the D_{32} ratio first decreases and then sharply increases at the smallest transmission. These unexpected evolutions of diameter ratio are due to a combination of vignetting and multiple light scattering effects. To illustrate this, Fig. 5 compares the full and half-spray drop-size distributions obtained at the smallest transmission. This figure shows that the tail of the full-spray distribution is below the one of the half-spray distribution, which evidences the impact of light multiple scattering. Note that the half-spray measurement (T'_{min} < 40%) may be also affected by light multiple scattering. On the other side of the distribution, the small-drop population of the full-spray measurement is less

than the one of the half-spray measurement. This difference is due to vignetting effects. The diameter ratios greater than 1 when 14% < T_{min} < 40% reveal that vignetting is more effective than light multiple scattering (see Fig. 6).
Second, we look at the series of coefficients $\kappa_i(T)$ defined by:

$$\kappa_i\left(T_{\min}\right)=\frac{I_i\left(T_{\min}\right)}{I_i\left(T'_{\min}\right)} \qquad i=10,11,...,35 \tag{1}$$

where i denotes the diode number, and $I_i(T_{min})$ and $I'_i(T_{min})$ is the normalized light intensity distribution of the full-spray measurement and the corresponding half-spray measurement, respectively. Fig. 6 shows the evolution of the coefficients $\kappa_i(T_{min})$ with T_{min} for a few diodes. For T_{min} > 20%, $\kappa_i(T_{min})$ are rather independent of the transmission. They are equal to 1 for diodes 10–34 and less than 1 for diode 35. This latter result is the manifestation of vignetting effects. Note that the influence of these effects on the intensity collected by diode 34 is negligible. For low transmission (less than 20%), κ_i becomes dependent on the transmission. The variation of κ_i with the transmission is a function of the diode. For internal diodes (up to the 22nd diode), κ_i decrease as T_{min} decreases whereas for the external diodes (from the 28th to the 35th diodes), κ_i increases as T_{min} decreases. Such variations of the coefficients κ_i are those expected from light multiple scattering effects. However, as discussed above, vignetting effects compensate light multiple scattering effects and the measurements must be corrected from both effects.

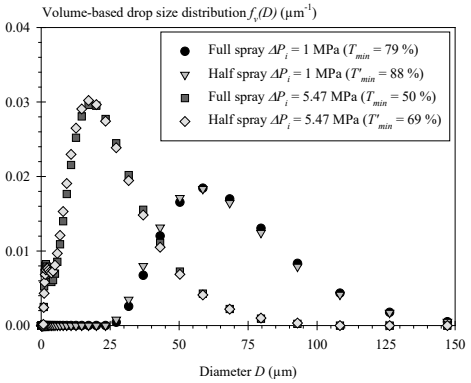

Fig. 3 Comparison between full and half spray drop-size distributions (ΔP_i = 1 MPa and 5.47 MPa).

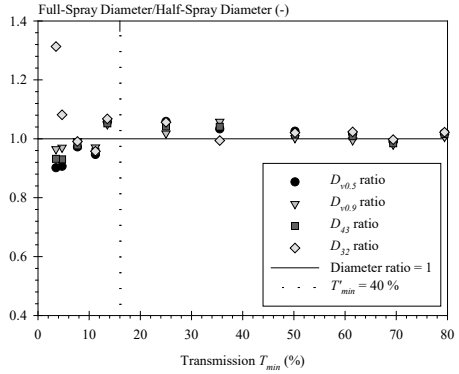

Fig. 4 Evolution of full-spray diameter/half-spray diameter ratio as a function of the transmission T_{min}.

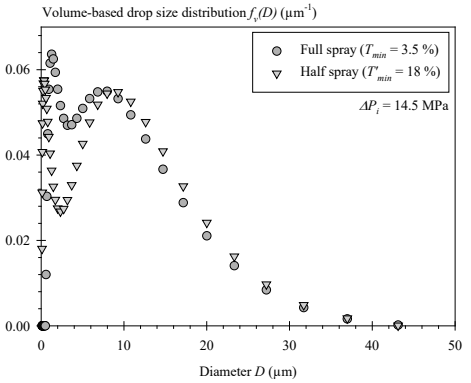

Fig. 5 Comparison between full-spray and half-spray drop-size distributions at ΔP_i = 14.5 MPa.

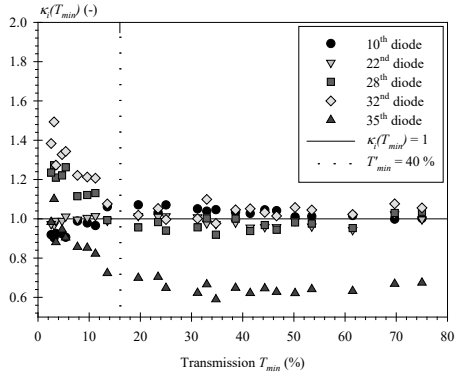

Fig. 6 Evolution of κ_i as a function of the full-spray minimum transmission. Influence of the diode.

3.2 Multiple light scattering and vignetting correction procedure

A corrected intensity distribution $\widetilde{I}_i(T)$ is calculated from the full-spray intensity distribution $I_i(T)$ by the relation:

$$\widetilde{I}_i(T)=\frac{I_i(T)}{\widetilde{\kappa}_i(T)} \tag{2}$$

introducing the correction factor series $\widetilde{\kappa}_i(T)$. If the half-spray measurement is not affected by multiple scattering, the corrected intensity $\widetilde{I}_i(T)$ must be equal to the intensity $I_i(T')$, i.e., $\widetilde{\kappa}_i(T)=\kappa_i(T)$ in Eq. (1). Note that this correction factor series also corrects from vignetting effects. Now, if the half-spray measurement is affected by multiple scattering

effects, the intensity distribution $I_i(T')$ requires to be corrected. However, the correction factors series for the half-spray measurements is unknown.

Light multiple scattering effects are mainly dependent on the transmission as well as on the spray characteristics [3-5]. However, in agreement of Gülder [3] and Felton [4] conclusions, the influence of the size parameter on the multiple light scattering effects is negligible. Using Felton et al.'s results (dispersion parameter), the error made for the corrected span factor is less than 10%. In our work, we found that the evolutions of the span factor of the full and half-spray measurement as a function of their transmission are very much alike. Therefore, we assume that the light multiple scattering effects are mainly dependent on only the transmission and that the same correction factor series can be used for the full and half-spray intensity distributions. Since vignetting never affects half-spray measurements, the corrected intensity distribution $\widetilde{I}_i(T)$ can be rewritten as:

$$\widetilde{I}_i(T) = \frac{a_i I_i(T')}{\widetilde{\kappa}_i(T')} \qquad \text{where} \qquad a_i = \lim_{T \to 100} \left(\kappa_i(T)\right) \tag{3}$$

In this work, $a_i = 1$ for all diodes except for diode 35 where $a_i = 0.64$. The series of correction factors $\widetilde{\kappa}_i(T)$ can be derived from Eqs. (1)–(3). By applying it for successive values of the transmission, it comes:

$$\widetilde{\kappa}_i(T) = a_i \prod_{j=0}^{n} \frac{\kappa_i\left((T)^{1/2^j}\right)}{a_i} \tag{4}$$

When multiple scattering effects do not affect the half-spray measurement, the first term of the series is required only, i.e., $n = 0$ because the successive terms of the series for $n > 0$ are equal to 1. When the half-spray measurement has to be corrected once, the two first terms of the series are required, i.e., $n = 0$ and 1, the series terms for higher n being all equal to 1. Therefore, the application of Eq. (4) requires a parameter n high enough so that the last term of the series in the right-hand side of the equation is equal to 1. This condition is always satisfied when $T^{1/2n} > 0.95$.

The correction factor series given by Eq. (4) is for full-spray measurements only. The light intensity distributions were unexploitable when $\Delta P_i > 14.5$ MPa ($T < 3.5\%$). However, for greater ΔP_i (between 15 MPa and 20 MPa) half-spray measurements are still possible. For half spray measurements, Eq. (4) is divided by a_i since vignetting does not affect.

To simplify the calculation of the correction factor given by Eqs. (4) for any T, the coefficients κ_i in Eq. (1) are modeled using the following expression:

$$\kappa_i(T) = a_i - \left(a_i - \kappa_i(0)\right)e^{\gamma_i T} \tag{5}$$

where a_i are defined by Eq. (3) and are obtained from Fig. 6. For each diode i, $\kappa_i(0)$ and γ_i have to be determined, namely,. This is achieved by rewriting Eq. (5) as $\ln\left(\left|a_i - \kappa_i(T)\right|\right) = \ln\left(\left|a_i - \kappa_i(0)\right|\right) + \gamma_i T$. This is the linear dependence expressed. For each diode, the slope of the linear regression gives the parameter γ_i and the ordinate for $T = 0$ returns the parameter $\kappa_i(0)$. Thus, the corrections factor series in Eq. (4) is calculated using the analytical expression of the coefficients $\kappa_i(T)$ in Eq. (5) and paying attention that the parameter n satisfies the condition $T^{1/2n} > 0.95$. As an illustration, the resulting coefficient series $\widetilde{\kappa}_i(T)$ (Eq. (4)) is shown in Fig. 7 for selected diodes.

The correction process developed here is actually a generalization of the procedure proposed by Boyaval and Dumouchel [6] that consisted in a double correction only, i.e., $n = 1$ in Eq. (4).

The nth order correction procedure is now applied to evaluate the limit transmission under which light multiple scattering affects the measurements. This can be achieved by determining the vignetting-free full-spray diameter/actual-spray diameter ratios (D_{32}, D_{43}, $D_{v0.5}$ and $D_{v0.9}$) as a function of the transmission as shown in Fig. 8. The full-spray measurements are corrected from vignetting effects only by dividing the intensity collected by each diode i by a_i. The results show that light multiple scattering effects start when $T_{min} < 40\%$ as seen by a decrease of D_{32} and $D_{v0.5}$. For $D_{v0.9}$ ratio, it starts decreasing when $T_{min} < 10\%$. These behaviors agree with the other work [7]. This limit is identical to many previous investigations, giving credit to the empirical correction procedure developed here.

We now examine the influence of light multiple scattering on spray drop-size distribution. The series of Fig. 9 compares the vignetting-free full-spray drop-size distribution with the actual-spray drop-size distribution resulting from the application of the nth order correction procedure. These figures show that the vignetting-free distribution is always left shifted compared to the actual distribution. This behavior corresponds to the expected influence of multiple light scattering. Fig. 9 also shows that the Malvern correction algorithm always overcorrects the measurements. This is due to the fact that the model on which this correction algorithm is based assumes isolated particle light scattering and spray characteristics (concentration and drop-size distribution) uniformly distributed in space [8, 9], which is not the case here. In conclusion, it is not recommended to use the Malvern correction algorithm for the present sprays.

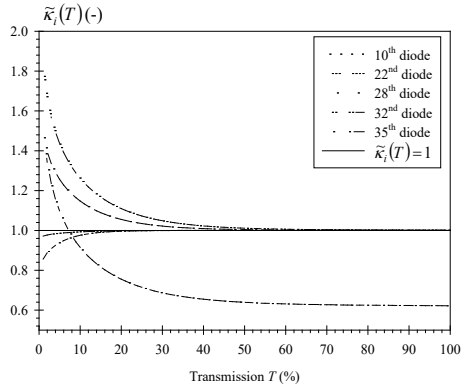

Fig. 7 Evolution of the correction factors $\tilde{\kappa}_i(T)$ (Eq. (4)) as a function of the full spray transmission T.

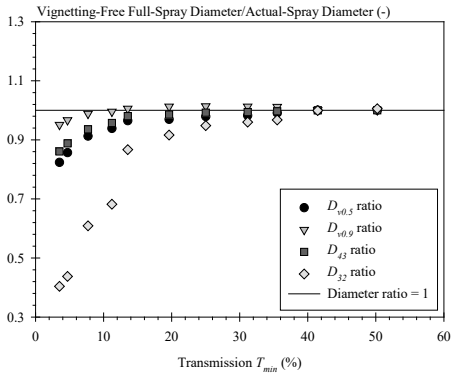

Fig. 8 Evolution of vignetting-free full-spray diameter/actual-spray diameter ratio as a function of the transmission T_{min}.

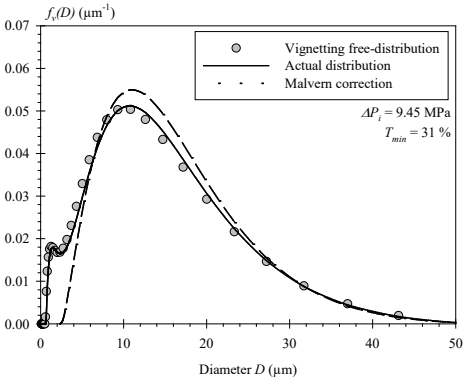

(a) ΔP_i = 9.45 MPa

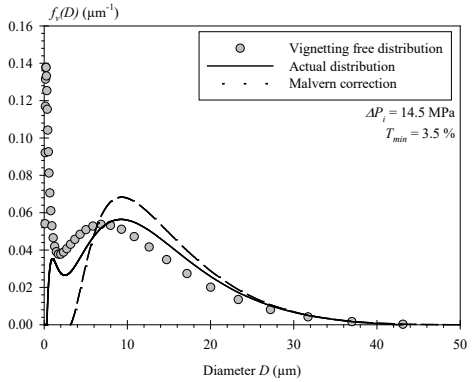

(b) ΔP_i = 14.5 MPa

Fig. 9 Comparison between the vignetting-free full-spray drop-size distribution, the actual-spray drop-size distribution and the drop-size distribution obtained from the application of the Malvern correction algorithm.

3.3. Example of applications

In this section, applications of the nth order correction procedure are performed to determine and investigate the drop-size distribution of the spray produce by the high-pressure GDI injector. Fig. 10 shows a series of volume-based drop-size distributions for an injection pressure ranging from 10 MPa to 20 MPa. These distributions are those obtained at the minimum transmission. At 10 MPa, the distribution is mainly mono-modal. When the injection pressure increases, the drop-size distribution shifts towards the small-drop population and a second peak develops in the 2 µm diameter region. The height of this peak increases with the injection pressure. As mentioned above, the atomization mechanism of the conical sheet issuing from the injector involves several liquid structures such as longitudinal ligaments and thin liquid lamellas. These liquid structures and their respective atomization mechanism have different characteristic length scales and are likely to produce distinct drop populations. One of the important specifications a GDI spray must fulfill is the absence of 45 µm drops. With the present GDI injector used with a 63% needle stroke energy, this condition is reached for injection pressures greater than 15 MPa.

The diagnostic with the Spraytec is able to follow the drop-size distribution temporal evolution during one injection with the maximum resolution of 0.1 ms. An example of this is shown in Fig. 11 for ΔP_i = 20 MPa by using the time step of 0.4 ms. The temporal evolution of the transmission is plotted also. This figure shows that the drop-size distribution is bi-modal all over the time. Between 2 ms and 4 ms after the injection command, the small-drop population mode is the most developed whereas the transmissions are smallest, which denotes the passage in the measurement volume of a high-density spray. Thus, the drop-size distributions measured during this time interval characterize the greatest proportion of injected liquid volume. After 5 ms, the drop-size distribution moderately varies whereas the transmission continuously increases. This characterizes the cloud of drops in suspension after the passage of the main spray.

The result shown in Fig. 11 was obtained from measurements averaged on 25 injections. The averaging process was a necessary step to develop a statistically representative correction procedure. However, this correction procedure can be applied on individual injection measurements to give the cycle-to-cycle variations of the drop-size distribution as shown in Fig. 12.

4. CONCLUSION

This work details a practical use of a laser-diffraction technique to characterize spray drop-size distribution. The phenomena that can affect the measurement are the beam steering, the vignetting and the light multiple scattering effects. The present experimental protocol includes the identification of the presence of these phenomena and an empirical correction procedure for light multiple scattering and vignetting effects. This correction procedure allows whole drop-size distribution to be determined instead of a limited number of spray characteristics. The application of the nth order correction procedure reported that light multiple scattering effects are effective when $T < 40\%$. This limit agrees with previous experimental results and thus gives credit to the correction model. Furthermore, it was demonstrated that the Malvern light multiple scattering algorithm is not adapted for the present sprays especially when the transmission is less than 30%. The combination of the Spraytec performances and of the present correction procedure allows spray drop-size distribution to be measured for injection pressure as high as 20 MPa and temporal evolution of the drop-size distribution during an injection to be investigated. Furthermore, it is important to emphasize that the determination of cycle-to-cycle temporal variations of the spray drop-size distribution is possible. This experimental protocol can be reproduced with ease on sprays produced from the disintegration of conical liquid flow as often encountered in GDI application.

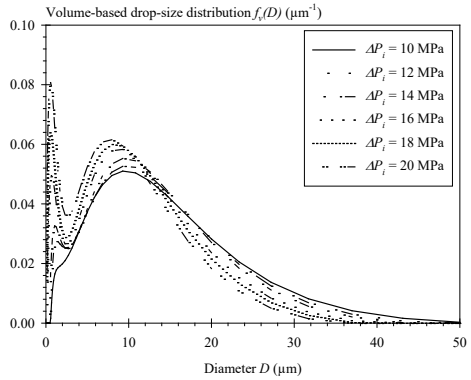

Fig. 10 Evolution of the drop-size distribution as a function of the injection pressure.

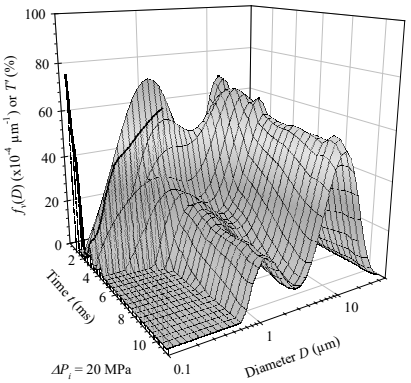

Fig. 11 Temporal evolution of the drop-size distribution and of the transmission during one injection (ΔP_i = 20 MPa).

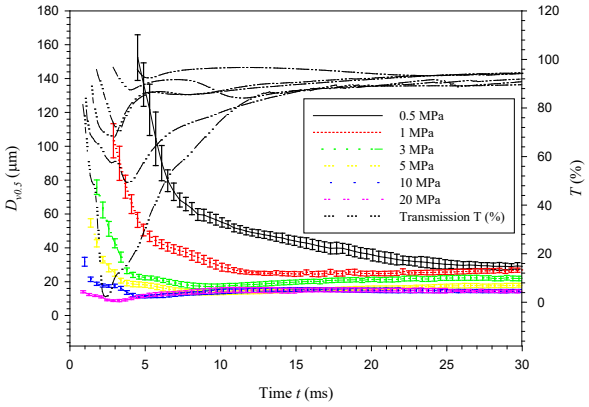

Fig. 12 Variation from cycle to cycle.

5. REFERENCES

[1] Corcoran, T.E., Hitron, R., Humphrey, W., Chigier, N. (2000) Optical measurement of nebulizer sprays: a quanti tative comparison of diffraction, phase Doppler interfero metry, and time of flight techniques, *J. Aerosol Sci.*, **31**, pp. 35–50.

[2] Boyaval, S., Dumouchel, C. (2001) Investigation on the drop size distribution of sprays produced by high-pressur e swirl injector. Measurements and application to the ma ximum entropy formalism, *Part. Part. Syst. Char.*, **18**, p p. 33–49.

[3] Gülder, O.L. (1990) Multiple scattering effects in dense spray sizing by laser diffraction. *Aerosol Sci. Technol*., **1 2**, pp. 570–577.

[4] Felton, P.G., Hamidi, A.A., Aigal, A.K. (1985) Measure ment of drop size distribution in dense sprays by laser dif fraction, *Proceedings of the ICLASS-85*, London, Englan d, Paper IVA/4/1.

[5] Dodge, L.G. (1984) Change of calibration of diffraction -based particle sizers in dense sprays, *Opt. Eng.*, **23**, pp. 626–630.

[6] Boyaval, S., Dumouchel, C. (2001) Investigation on the drop size distribution of sprays produced by high-pressure swirl injector. Measurements and application to the maximum entropy formalism, *Part. Part. Syst. Char.*, **18**, pp. 33 –49.

[7] Paloposki, T., Kankkunen, A. (1991) Multiple scattering and size distribution effects on the performance of a laser diffraction particle sizer, *Proceedings of the International Conference on Liquid Atomization and Spray Systems*, IC LASS'91, Gaithersburg, USA, Paper 46, pp. 441–448.

[8] Hirleman, E.D. (1988) Modeling of multiple scattering effects in Fraunhofer diffraction particle size analysis, *Part. Part. Syst. Char.*, **5**, pp. 57–65.

[9] Hirleman, E.D. (1990) A general solution to the inverse near-forward scattering particle sizing problem in multiple scattering environment: Theory, *Second International Congress on Optical Particle Sizing*, Tempe, Arizona, USA, pp. 159–168.